EUROPEAN ORGANIZATION FOR NUCLEAR RESEARCH

THE REAL PART OF THE FORWARD PROTON PROTON SCATTERING AMPLITUDE MEASURED AT THE CERN INTERSECTING STORAGE RINGS

U. Amaldi, G. Cocconi, A.N. Diddens, R.W. Dobinson,
J. Dorenbosch*), W. Duinker, D. Gustavson**),
J. Meyer, K. Potter, A.M. Wetherell

CERN, Geneva, Switzerland

A. Baroncelli, C. Bosio

Istituto Superiore di Sanità and
Istituto Nazionale di Fisica Nucleare, Rome, Italy

ABSTRACT

The real part of the proton proton elastic scattering amplitude has been determined from its interference with the Coulomb amplitude at total centre-of-mass energies up to 62 GeV. The observed steady increase of ρ with energy indicates that the total proton proton cross section continues to increase well beyond this energy.

Geneva
November 1976

(Submitted to Physics Letters)

---

*) Visitor from Zeeman Laboratory, Amsterdam, Netherlands

**) On leave from SLAC, Stanford, California

This letter presents the results of measurements of elastic proton proton scattering at very small four-momentum transfer ($0.001 < |t| < 0.020$ GeV^2). The measurements have been performed at the CERN Intersecting Storage Rings (ISR), for beam momenta of 15.4, 22.5, 26.7 and 31.5 GeV/c.

In the t range studied in this experiment the differential cross section is determined by both the Coulomb and the nuclear scattering amplitudes:

$$d\sigma/dt = \pi|f_C+f_n|^2 \qquad (1)$$

Coulomb scattering is the dominant process at the low end of the t range. Its amplitude is given by the expression:

$$f_C = -2\alpha \frac{G^2(t)}{|t|} \exp(i\alpha\Phi) \qquad (2)$$

where α is the fine structure constant, and G(t) is the proton electromagnetic form factor, for which the usual dipole form has been used[1]. In equation 2:

$$\alpha\Phi = \alpha\{\ln(0.08/|t|)-0.577\} \qquad (3)$$

is the phase of the Coulomb amplitude, as calculated by West and Yennie[2] and by Locher[3]. For the nuclear amplitude the familiar form:

$$f_n = \frac{\sigma_{tot}}{4\pi} (\rho+i) \exp(\tfrac{1}{2}bt) \qquad (4)$$

is used. The real and the imaginary parts are assumed to have the same exponential t dependence, and spin effects are neglected. Justifications of these assumptions have been given in reference [4].

The real part can be determined from the interference that occurs between the Coulomb and the nuclear amplitude. The interference term in the differential cross section varies as t^{-1}, so that it can be distinguished from the Coulomb contribution with its steep t^{-2} dependence, and from the almost flat nuclear part. At medium energies the ratio ρ between the real

and the imaginary part is negative. Earlier measurements performed by this collaboration indicated that ρ could become positive at higher energies[4]. This was subsequently established by measurements at Fermilab[5]. The present experiment measures ρ at the highest energies attainable at the present time.

The angular distribution of protons, scattered in the vertical plane, was measured with an apparatus installed at an intersection in the ISR (Fig. 1). Four scintillator hodoscopes were placed in thin-walled movable sections of the ISR vacuum chamber, that made it possible to move the scintillators close to the circulating beams. The hodoscopes were assembled in three layers; a stack of twenty-four 2 mm high scintillators that defined the vertical component of the scattering angle, an array of seven vertical 4 mm wide fingers that determined the horizontal component, and behind them a single trigger counter. The four hodoscopes were combined in two pairs, AB and CD (Fig. 1), such that, for elastic collisions, if one proton hit a hodoscope the other proton traversed the hodoscope conjugate to the first one. A trigger was generated only if both hodoscopes of a pair were traversed by a particle. For all triggers a pattern unit recorded which elements had fired, the pulse heights in all counter elements were measured, and the time-of-flight difference between the hits in the two hodoscopes was determined. A CAMAC system and a small on-line computer were used for data collection and storage on magnetic tapes.

To be able to move the counters well into the region where Coulomb scattering dominates, beams with a height and a width of only a few millimetres were essential. Therefore the ISR was operated using the Terwilliger focussing scheme, thus superimposing the equilibrium orbits for different momenta in the intersection region[6]. In addition the halos of the beams were scraped off at injection time and at regular intervals during data taking. Beams of a few ampères were obtained with cross sections twice as low and ten times as narrow as under normal running conditions. This made it possible to bring the counters as close as 9 mm to the beam axis, where they detected protons scattered at angles of 1 mrad. A source length as small as 35 mm FWHM could be obtained.

In the off-line data analysis the measured pulse heights were used to resolve the multiple hit ambiguities caused by delta rays, and time-of-flight cuts were made to correct for the contribution of random coincidences. The events were accumulated in two sets of 24 by 24 matrices, each set corresponding to a pair of hodoscopes. Events where the i-th stack element in one hodoscope and the j-th elements of the other one were hit were added to the (i, j)-th element of these matrices. In Figure 1 d a typical coincidence matrix is reproduced. The narrow ridge, containing the collinear elastic events, can clearly be identified. The small inelastic background can be estimated from the region far from this ridge.

A Chi squared minimization was performed on the well populated matrix elements. The free parameters in the fit were ρ, the height and width of the source, the three-dimensional coordinates of the centre of the source, an overall normalization constant, and the vertical distances between hodoscopes A and C and between B and D. The total proton proton cross section and the slope of the elastic diffraction peak were put into the fit as fixed parameters. The fitting procedure has been tested extensively on Monte Carlo generated events.

Two checks could be made on the results of the fits. The multiwire proportional chamber telescope shown in Figure 1 a was used to observe particles scattered at 90 degrees. From these data the projection of the intersection region in the vertical plane could be reconstructed. In this way independent estimates were obtained of the width and the longitudinal position of the intersection region that agreed with the fitted ones. The uncertainty in the results of the fit for the vertical distances corresponded to a resolution in the angular position of the hodoscopes better than 0.01 mrad. The fitted values could be compared with values obtained from the mechanical system that moved the hodoscopes. The accuracy of these movements was about 0.1 mm. Within this accuracy the results of both determinations were in good agreement with each other. If the values obtained from the telescope or from the mechanical system were used as fixed parameters in the fit, ρ did not change significantly.

The sources of errors in the determination of ρ are listed in table 1. The first column shows the uncertainties corresponding to an

increase of Chi squared by one, taking into account the correlations between all free parameters. The uncertainties in column 4 coming from the analysis were estimated by varying the number of matrix elements that were considered in the fit. Table 2 shows the number of events that was used in the fit, the valuesof the total cross section and the slope that have been put in, and the final values obtained for ρ, as a function of the centre-of-mass energy, $\sqrt{s}$. The errors in ρ appearing in tables 1 and 2 are point-to-point errors. In addition there is a scale error of about 0.015, common to all determinations of ρ, which arises from the uncertainty in the phase of the Coulomb amplitude (3)[2]. The cross section and the slope were obtained from interpolations of previous measurements[4),7), 8)].

At beam momenta of 31.5 GeV/c a new measurement of the slope was performed, moving the hodoscopes to a distance of 40 mm from the beam axis, where they detected elastically-scattered protons with four-momentum transfers between 0.02 and 0.09 GeV^2. The data were perfectly fitted by an exponential behaviour of the nuclear amplitude, with a slope parameter b equal to 13.4 ± 0.2.

From the distributions in the matrices the elastic differential cross section has been evaluated. Figure 2 a shows the result at ISR beam momenta of 26.7 + 26.7 GeV/c. Together with this cross section we display the quantity R, defined as:

$$R = \frac{d\sigma/dt \text{ (measured)}}{d\sigma/dt \text{ (for } \rho=0)} - 1. \qquad (5)$$

Figure 2 b shows R for all energies. It demonstrates a considerable destructive interference. The goodness of the fit supports the parametrization of the differential cross section contained in the expressions (1) to (4).

The real part of the scattering amplitude is connected to the absorptive part through a dispersion relation. Under the assumption that unitarity and crossing symmetry are valid, one obtains the once-subtracted dispersion relation as given by Söding[9]. In the energy range of this experiment, where one is far from the unphysical region, it can be approximated by:

$$\mathrm{Re}\, f_+(E) = C + \frac{mE}{8\pi^2}\int_m^\infty dE' \left[\frac{\sigma_+(E')}{E'-E} - \frac{\sigma_-(E')}{E'+E}\right] \qquad (6)$$

where C is a constant and σ_+ and σ_- are the proton proton and the anti-proton proton total cross sections, which we have parametrized as:

$$\sigma_{\pm} = C_1\, E_{lab}^{-\nu_1} \pm C_2\, E_{lab}^{-\nu_2} + \sigma_\infty \qquad (7)$$

$$\sigma_\infty = B_1 + B_2\, (\ln s)^\gamma \qquad (8)$$

At high energies the assumed cross sections become equal and behave like a power of the logarithm of s. The constants of this parametrization and the constant C in formula (6) have been determined by fitting existing total cross section data[8),10),11)] and at the same time the data for ρ from the present experiment and from refs. 4 and 12 using dispersion relation (6). The systematic errors in the data have been taken into account in this fit. For the constants that determine the cross section behaviour we find the values (cross sections in mb and energies in GeV):

$$C_1 = 41.9 \pm 1.1$$
$$C_2 = 24.2 \pm 1.1$$
$$\nu_1 = 0.37 \pm .03$$
$$\nu_2 = 0.55 \pm .02$$
$$B_1 = 27.0 \pm 1.0$$
$$B_2 = 0.17 \pm .08$$
$$\gamma = 2.10 \pm .10$$

The result of this fit is shown as full curves in Figure 3 a and 3 b. The shaded areas around these curves represent the regions within which the proton proton and the anti-proton proton cross sections and ρ can differ from the best fit, if one allows the Chi squared of the minimization to increase by one unit. We conclude that the results of the present experiment together with previously measured data indicate that the proton-proton and the antiproton-proton total cross-sections should rise at least up to equivalent laboratory energies of 40 TeV, where they should reach a value of about 55 mb.

We would like to thank the personnel of the ISR Division for having provided the precise and stable beams vital for this experiment and for many other contributions. In particular we thank J.C. Brunet, J.C. Godot, E. Jones and G. Rollinger for their work on the construction of the special vacuum chamber, and E. Sbrissa and J.M. Schmitt who developed the system that controlled the movements of the hodoscopes. We are grateful to C. Busi for help in the data analysis and to R. Donnet and M. Ferrat for their excellent technical support. Thanks are also due to J. Allaby for useful discussions and to O. Bottner and R. Rüsch who worked in our collaboration as CERN summer students.

Table 1

Sources of errors in the evaluation of ρ. The errors assumed for the total cross section and the slope appear in table 2

ISR momenta (GeV/c)	From fit	From σ_{tot}	From b	From analysis	Overall error
15.4 + 15.4	0.0070	0.0045	0.0027	0.0060	0.011
22.5 + 22.5	0.0050	0.0027	0.0055	0.0070	0.011
26.7 + 26.7	0.0063	0.0027	0.0051	0.0046	0.010
31.5 + 31.5	0.0074	0.0025	0.0060	0.0040	0.011

Table 2

Number of events, values used for the total cross section and the slope, obtained from *a smooth fit to* existing data, and the final values obtained for ρ

$\sqrt{s}$ (GeV)	Number of events	σ_{tot} (mb)	Slope	ρ
30.6	774000	40.1 ± 0.4	12.2 ± 0.3	0.042 ± 0.011
44.7	2478000	41.7 ± 0.4	12.8 ± 0.3	0.062 ± 0.011
52.9	2752000	42.4 ± 0.4	13.1 ± 0.3	0.078 ± 0.010
62.4	2290000	43.1 ± 0.4	13.3 ± 0.3	0.095 ± 0.011

References

1) D.H. Coward et al., Phys. Rev. Lett. 20 (1968) 292.

2) G.B. West and D.R. Yennie, Phys. Rev. 172 (1968) 1413.

3) M.P. Locher, Nucl. Phys. B2 (1967) 525.

4) U. Amaldi et al., Phys. Lett. 43B (1973) 231.

5) V. Bartenev et al., Phys. Rev. Lett. 31 (1973) 1367.

6) K.M. Terwilliger, Proc. Intern. Conf. on High Energy Accelerators (CERN, 1959) 53.

7) U. Amaldi et al., Phys. Lett. 36B (1971) 504.
G. Barbiellini et al., Phys. Lett. 39B (1972) 663.
V. Bartenev et al., Phys. Rev. Lett. 31 (1973) 1088.

8) CERN-Pisa-Rome-Stony Brook Collaboration, Phys. Lett. 62B (1976) 460.

9) P. Söding, Phys. Rev. Lett. 19 (1967) 857.

10) W. Gailbraith et al., Phys. Rev. 138B (1965) 913.
G. Bellettini et al., Phys. Lett. 14 (1965) 164.
K.J. Foley et al., Phys. Rev. Lett. 19 (1967) 857.
S.P. Denisov et al., Phys. Lett. 36B (1971) 528.

11) A.S. Carroll et al., Phys. Lett. 61B (1976) 303.

12) K.J. Foley et al., Phys. Rev. Lett. 19 (1967) 857.
G.G. Beznogikh et al., Phys. Lett. 39B (1972) 411.

Figure captions

Fig. 1 The apparatus used in this experiment. The positions of the movable indents and the 90 degrees telescope can be seen in the top and side view of the intersection (Fig. a). The indents and the structure of the scintillator hodoscope are shown in more detail in Figs. b and c. A typical coincidence matrix is displayed in Fig. 1.d. The collinearity of elastic collisions is exhibited by a strong accumulation around the main diagonal of the matrix.

Fig. 2.a The differential cross section fitted to experimental data at beam momenta of 26.7 + 26.7 GeV/c (full line), and the one expected for $\rho = 0$ (dashed curve).

2.b The quantity R, (equation (5) in the text) for all beam momenta. The solid curves are the best fits to the data.

Fig. 3 The top part of this figure shows the data obtained for ρ in this experiment, together with data at lower energies[4),12)]. The full curves are the result of a fit, simultaneously performed on total cross section data[8),10),11)] and on the data for ρ. The shaded areas represent the one standard deviation regions for ρ and the cross sections. The boundaries of these regions were obtained by changing the high energy behaviour of the cross sections (eq. 8) in such a way that the Chi squared of the fit increased by one.

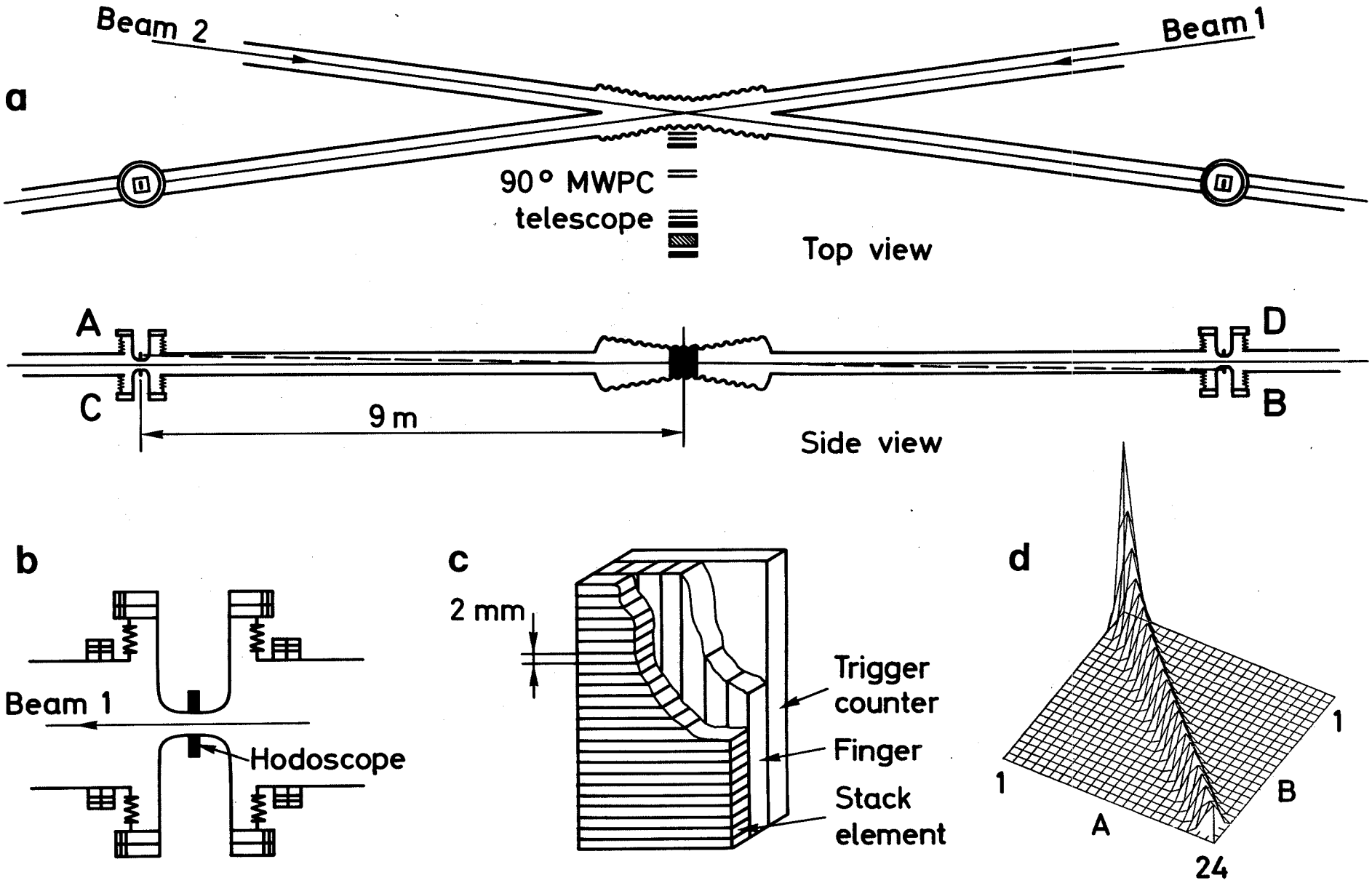
a
Beam 2
Beam 1
90° MWPC
telescope
Top view
A
C
D
B
9 m
Side view
b
Beam 1
Hodoscope
c
2 mm
Trigger
counter
Finger
Stack
element
d
1
1
B
A
24

Figure 1

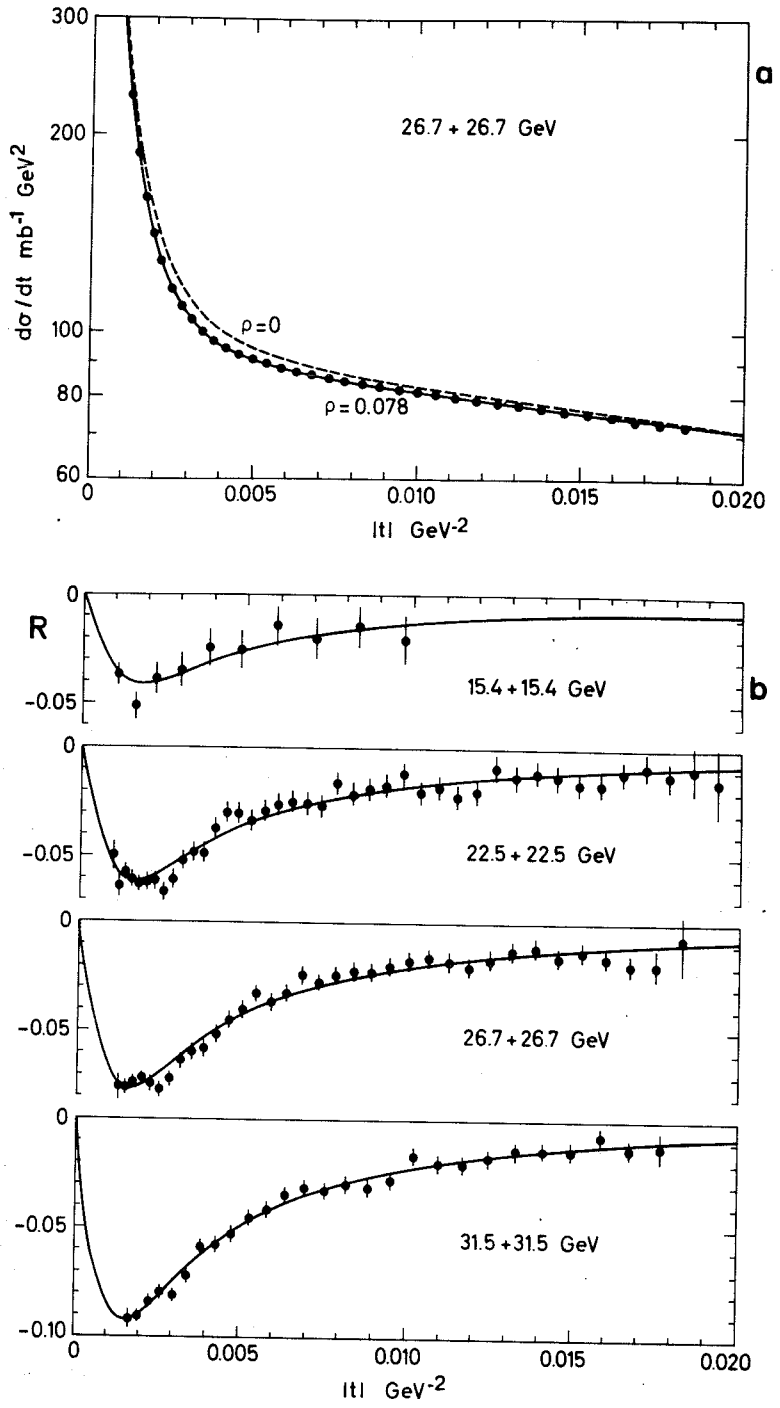
300
200
100
80
60
dσ/dt mb⁻¹ GeV²
26.7 + 26.7 GeV
a
ρ=0
ρ=0.078
0
0.005
0.010
0.015
0.020
|t| GeV⁻²
R
0
-0.05
15.4 + 15.4 GeV
b
22.5 + 22.5 GeV
26.7 + 26.7 GeV
31.5 + 31.5 GeV
-0.10
0
0.005
0.010
0.015
0.020
|t| GeV⁻²

Figure 2

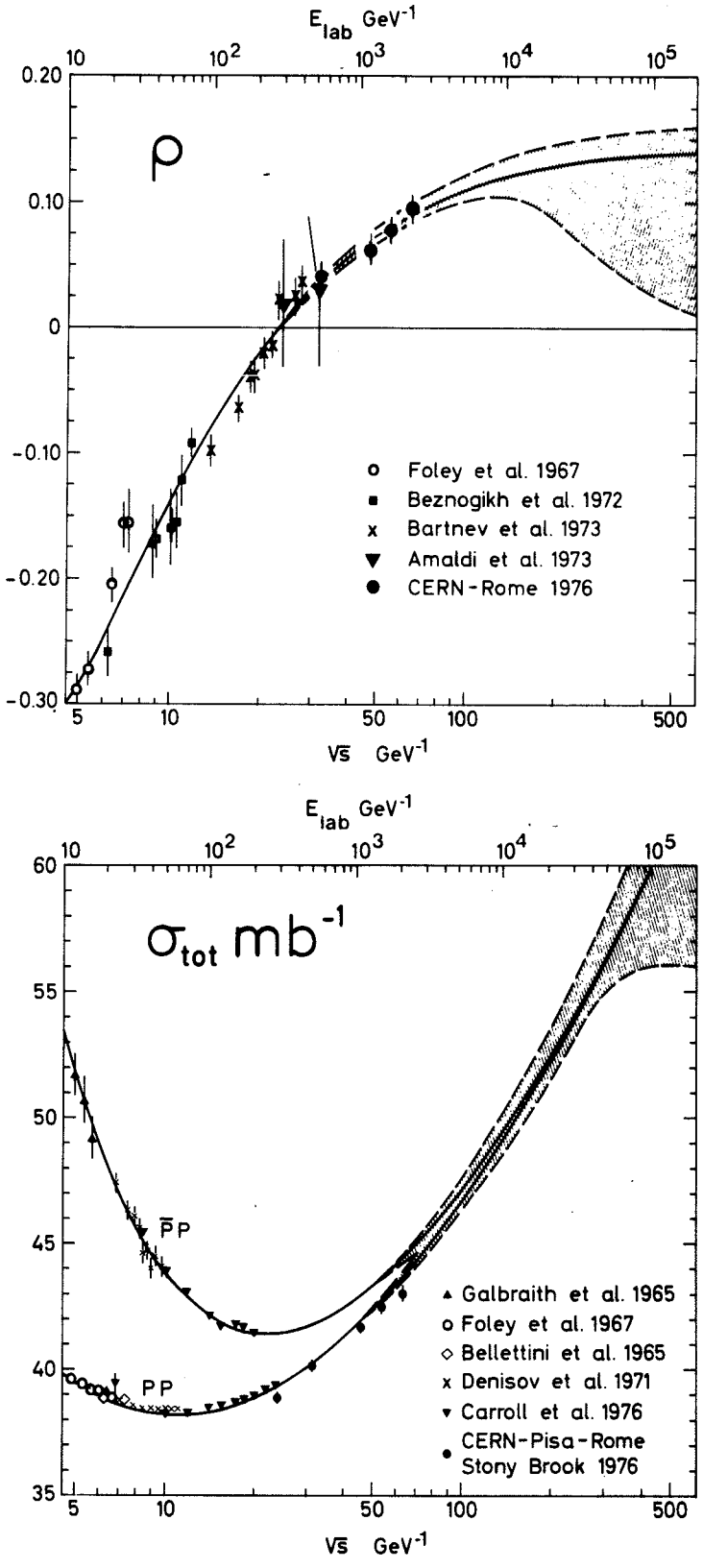
E_lab GeV^-1
10
10^2
10^3
10^4
10^5
0.20
0.10
0
-0.10
-0.20
-0.30
ρ
Foley et al. 1967
Beznogikh et al. 1972
Bartnev et al. 1973
Amaldi et al. 1973
CERN-Rome 1976
5
10
50
100
500
√s GeV^-1
E_lab GeV^-1
10
10^2
10^3
10^4
10^5
60
55
50
45
40
35
σ_tot mb^-1
P̄P
PP
Galbraith et al. 1965
Foley et al. 1967
Bellettini et al. 1965
Denisov et al. 1971
Carroll et al. 1976
CERN-Pisa-Rome Stony Brook 1976
5
10
50
100
500
√s GeV^-1

Figure 3